Copy 6
RM E54I20

NACA RM E54I20

RESEARCH MEMORANDUM

INVESTIGATION OF COMPRESSIBLE FLOW MIXING LOSSES OBTAINED DOWNSTREAM OF A BLADE ROW

By Warner L. Stewart

Lewis Flight Propulsion Laboratory
Cleveland, Ohio

NATIONAL ADVISORY COMMITTEE
FOR AERONAUTICS

WASHINGTON
December 9, 1954

NACA RM E54I20

[redacted]

NATIONAL ADVISORY COMMITTEE FOR AERONAUTICS

RESEARCH MEMORANDUM

INVESTIGATION OF COMPRESSIBLE FLOW MIXING LOSSES OBTAINED DOWNSTREAM OF A BLADE ROW

By Warner L. Stewart

SUMMARY

An investigation was conducted to determine the importance of the mixing loss downstream of a blade row with respect to blade profile loss for compressible flow conditions. Results of the analytical phase of the investigation indicated that increasing the blade exit velocities into the high subsonic and supersonic levels resulted in a relatively increased mixing loss, with this loss representing a sizable addition to the blade profile loss. For specified velocity level and blade profile loss, only secondary variations occurred in the mixing loss with respect to the blade exit flow angle. Comparison of the analytical results with those obtained in the experimental investigation of a transonic turbine stator indicated good agreement in the vicinity of the mean section where nominal two-dimensional flow conditions existed.

INTRODUCTION

The increased flow velocities through compressors and turbines have yielded important improvements in the performance characteristics of these units. For example, the use of transonic or supersonic flow velocities through compressors has resulted in a high pressure ratio per stage and a high specific weight flow (ref. 1). The increased flow velocities have also resulted in the attainment of increased specific weight flow and work output for turbines (ref. 2). However, in the application of these high-velocity turbomachines, it is important that high efficiencies be maintained. Thus, it is desirable to know the effect of the increased flow velocities on the various losses encountered.

One of the more important losses in compressors and turbines is the blade profile loss. Accompanying this loss and directly dependent upon it is the mixing loss that occurs downstream of the blade row. This mixing loss is a result of the nonuniformity of flow at the blade exit and has already been studied for incompressible flow to some degree. For example, the fundamentals were applied in reference 3 to study the effect of blade trailing-edge thickness on the blade losses.

[redacted]

This report presents the results of an investigation at the NACA Lewis laboratory of the effect of compressibility on the importance of the mixing loss occurring downstream of a blade row. Included is a two-dimensional analysis of the theoretical mixing loss as a function of the blade profile loss for a range of blade exit critical velocity ratios (ratio of flow velocity to that at a Mach number of 1) and a range of blade exit flow angles. Also, comparison of the analytical results is made with those obtained experimentally for the high-velocity stator used in the transonic turbine investigation of reference 2.

METHOD OF ANALYSIS

In the analytical phase of the investigation, two-dimensional flow conditions were specified. A description of the basic consideration involved can be made through use of figure 1, where a typical blade row is indicated. (All symbols are defined in appendix A.)

Station 0. - Station 0 represents the inlet to the blade row. It is assumed in the analysis that the flow at this station has a uniform total pressure p'_0. Although the blades in figure 1 have an entrance angle of zero degrees, any angle could be shown because the analytical method is independent of the blade entrance flow angle.

Station 1. - This station is located immediately downstream of the blade row. The flow is assumed to leave the blade at a constant angle α_1, with free-stream total pressure at this station equal to p'_0, and at a specified free-stream critical velocity ratio $(V/V_{cr})_{1,fs}$. The blade profile loss is assumed to result in a wedge cut in the total-pressure profile of width t and maximum depth equal to the free-stream dynamic head. This form of total-pressure profile was selected because similar profiles have been observed at the exit of high-velocity turbine stator blade rows. The profile as assumed might be questionable, in general, as it is a function of the blade boundary layer history. However, it is believed that the shape of the profile has only a secondary effect on the resulting mixing loss. As such, the trends of the analysis results presented herein can be considered generally valid. The static pressure at station 1 is also assumed to be uniform.

Station 2. - This station is located farther downstream of the blade row, where complete mixing is assumed to have taken place. The total pressure p'_2 is uniform and, of course, at a value less than p'_0.

The equations of continuity, momentum, and energy were used in determining the loss that occurs between stations 1 and 2. A derivation of these equations, as well as their use, is presented in appendix B.

In applying these equations, ranges of free-stream critical velocity ratio $(V/V_{cr})_{1,fs}$, blade exit flow angle α_1, and total-pressure wedge cut width t/s were selected. For any combination of these parameters, the total-pressure ratio $(p_1'/p_0')_p$ could be calculated. This total-pressure ratio across the blade row represents the blade profile loss. Then, using the equations of appendix B, the over-all total-pressure ratio p_2'/p_0' was computed. This total-pressure ratio includes not only the blade profile loss but also the mixing loss.

The analytical results will be presented in terms of a head loss coefficient $\bar{\omega}$ as well as in terms of the total-pressure ratio. In determining values of $\bar{\omega}$, the dynamic head at free-stream conditions at station 1 was used as a basis. Dynamic head is herein defined as the difference between the total and static pressures at a given point. The equations used in calculating the blade profile head loss $\bar{\omega}_1$ and the over-all head loss $\bar{\omega}_2$ are included in appendix B.

DESCRIPTION OF APPARATUS AND PROCEDURE

The apparatus used in the experimental phase of the investigation is shown in schematic form in figure 2. The blade row selected for this investigation was the stator used in the transonic turbine investigation of reference 2. The turbine had an outer diameter of 14 inches with a constant hub-tip ratio of 0.7. The rotor was replaced by a fairing piece as shown in figure 2. Station 2 corresponds to that station just downstream of the rotor when it is in place.

Surveys were taken at stations 1 and 2 with the turbine stator operating at approximately its design condition. These stations were located approximately 3/16 inch and 4 inches, respectively, downstream of the stator exit. The stator inlet conditions were maintained at nominal values of 32 inches of mercury absolute and 145° F. The total pressures at stations 1 and 2 were obtained in the form of a difference in inlet total pressure from that at station 0. In this way, any minor fluctuations in inlet total pressure would have a very small effect on the resulting pressure contours. The total pressure was measured through use of an automatic recording unit which traced loss in total pressure with respect to circumferential location for a given radius. Self-balancing miniature claw total-pressure probes were used as instrumentation. Static-pressure taps were also located on the inner and outer walls at all three stations.

RESULTS OF INVESTIGATION

Analytical Results

The results of the analytical investigation of the mixing loss occurring downstream of a blade row for the conditions assumed herein are presented in figure 3. Both the blade profile head loss coefficient $\bar{\omega}_1$ and the over-all head loss coefficient $\bar{\omega}_2$ are presented as a function of the total-pressure wedge cut width t/s. Values of critical velocity ratio $(V/V_{cr})_{1,fs}$ of 0.6, 1.0, and 1.4 and blade exit flow angle α_1 of 0°, 45°, and 75° are included as parameters.

Figure 3 indicates that, for a specified blade profile loss coefficient or wedge cut width and critical velocity ratio, the blade exit flow angle has only a secondary effect on the over-all head loss coefficient. Velocity level does affect the mixing loss to a much greater extent, as indicated by the increased difference between the over-all and blade profile loss coefficients as the critical velocity ratio is increased to high subsonic and supersonic values. For example, at $\bar{\omega}_1 = 0.06$, $(V/V_{cr})_{1,fs} = 0.6$, and $\alpha_1 = 45^\circ$, the over-all head loss coefficient $\bar{\omega}_2$ is 0.077. Thus, for this velocity level, approximately 30 percent additional total-pressure loss occurs as a result of mixing. At a critical velocity ratio of 1.4 for the same $\bar{\omega}_1$ and α_1, the over-all head loss coefficient $\bar{\omega}_2$ is 0.094, representing approximately 55 percent additional loss caused by mixing. Thus, it is indicated that the mixing downstream of the blade row represents a considerable addition to the blade profile loss and that this loss increases markedly with velocity level.

Figure 4 presents the results of the mixing loss analysis in terms of total-pressure ratios. The over-all total-pressure ratio p_2'/p_0' is presented as a function of the blade profile total-pressure ratio $(p_1'/p_0')_p$, with critical velocity ratio and blade exit flow angle shown as parameters. Of course, these curves show the same trends as those in figure 3. The angle is seen to have only a secondary effect, whereas increases in critical velocity ratio result in increases in the mixing loss.

Experimental Results

The turbine stator selected for the experimental phase of the investigation was the one designed for the transonic turbine investigation of reference 2, and as such had relatively high velocities at station 1.

In figure 5 is shown the variation in free-stream critical velocity ratio with radius at this station (station 1). This velocity ratio was obtained using the free-stream total pressure at station 1 assumed equal to that measured at station 0 and the static pressure measured at the inner and outer walls at station 1, assuming a linear variation of the static pressure with radius. It can be seen from the figure that the critical velocity ratio varies from 1.35 at the hub to 0.87 at the tip. This variation in critical velocity ratio at station 1 is used in conjunction with figure 4 and the circumferentially mass-averaged profile total-pressure ratio across the stator blade in computing the theoretical mixing loss downstream of the stator.

The contours of total pressure obtained from the surveys at station 1 are shown in figure 6, where the total-pressure ratio p_1'/p_0' is presented as a function of radial and circumferential position covering slightly over 1 blade pitch. Over the free-stream area the total-pressure ratio is over 0.99, indicating that the free-stream conditions are almost isentropic. The stator wake and core regions can also be observed.

As the flow continues downstream, the core and wake regions mix. The resultant total-pressure ratio contours at station 2 are indicated in figure 7. This figure shows that although gradients in the radial direction still occur, almost complete mixing in the circumferential direction is obtained. The pressure ratio p_2'/p_0' is greater than 0.96 over only a small region of the annulus. Near the hub and tip the loss tends to increase in comparison with that in the region of the mean section, with the greater increase near the hub. It can also be observed that complete mixing has not quite taken place near the tip. However, since the difference between the maximum and minimum pressure ratios in the circumferential direction is at the maximum about 4 points, very little additional mixing loss would be expected beyond this axial station. Comparison of figure 7 with figure 6 also indicates that additional loss has occurred between stations 1 and 2.

The values of p_1'/p_0' and p_2'/p_0' were mass-averaged circumferentially for each radial position surveyed. The resultant variation in total-pressure ratio with radius is shown in figure 8. Also included is the variation in the total-pressure ratio p_2'/p_0' obtained using the experimental results at station 1 and figure 4. In the region of the mean section, there is good agreement of the experimentally and analytically obtained total-pressure ratios after mixing. As the end walls are approached, losses greater than those predicted occur experimentally. This would be expected as the method of analysis is on a two-dimensional basis and as such does not consider the end wall effects occurring experimentally.

[redacted]

APPLICATION OF MIXING LOSS RESULTS TO EXAMPLE TRANSONIC TURBINE

The turbine of reference 2 will be used in this section as a typical high velocity turbomachine in illustrating the relative importance of the mixing loss in comparison with the over-all losses obtained.

From the velocity diagrams at the mean section presented in reference 2, the stator exit critical velocity ratio was specified to be 1.12 at a flow angle of approximately 60°. The rotor exit critical velocity ratio at this section was 1.02 at an angle of approximately 40°. The over-all pressure ratios for these two blade rows are 0.964 and 0.943, respectively, as determined by use of the measured blade profile total-pressure ratio of 0.975 across the stator (fig. 8) and an assumed value of 0.960 across the rotor along with figure 4 and the velocity diagram specifications. Thus for this high velocity turbine, the mixing loss represents an indicated addition to the profile loss of the order of 45 percent.

The total-pressure ratio across the turbine including the mixing loss alone computed from the figures just discussed is approximately 0.967. This pressure ratio represents a so-called unavailable energy of 1.18 Btu per pound as compared with an over-all unavailable energy obtained for this turbine of 3.44 Btu per pound. Thus the mixing loss in this form represents for this unit over 30 percent of the total loss. In terms of efficiency the loss represents of the order of 4 points for this unit.

The numbers used in this illustration are, of course, approximate; however, the values are believed representative of those actually obtained in the turbine. It should be further noted that the mixing loss computed in the illustration is less than that expected experimentally, because the mixing loss due to the end wall effects is not considered. Therefore, in view of the foregoing considerations, the example clearly emphasizes the possible importance of the mixing loss with respect to the over-all losses occurring in high-velocity turbomachinery.

SUMMARY OF RESULTS

An investigation of the effect of mixing downstream of a blade row was made for compressible flow conditions. The pertinent results of the investigation can be summarized as follows:

1. The results of the mixing loss analysis made on a two-dimensional basis indicated that increasing the blade exit velocities into the high subsonic and supersonic levels resulted in a relatively increased mixing loss, with this loss representing a sizable addition to the blade

profile loss. For specified velocity level and blade profile loss, only secondary variations in mixing loss with respect to blade exit flow angle were found to occur.

2. Results of surveys taken downstream of a high-velocity turbine stator indicated good agreement between the analytically and experimentally obtained mixing losses in the vicinity of the mean section where nominal two-dimensional flow conditions existed.

Lewis Flight Propulsion Laboratory
National Advisory Committee for Aeronautics
Cleveland, Ohio, September 16, 1954

APPENDIX A

SYMBOLS

The following symbols are used in this report:

g	acceleration due to gravity, 32.17 ft/sec^2
p	pressure, lb/sq ft
R	gas constant, ft-lb/(lb)($^\circ$R)
s	blade spacing, ft
T	temperature, $^\circ$F abs
t	tangential width of cut in total-pressure profile at station 1, ft
u	distance in tangential direction, ft
V	absolute gas velocity, ft/sec
w	weight flow, lb/sec
α	flow angle measured from axial direction, deg
γ	ratio of specific heats
ρ	gas density, lb/cu ft
$\bar{\omega}$	head loss coefficient based on free-stream dynamic pressure at station 1

Subscripts:

cr	conditions at Mach number of 1
fs	conditions in free stream or that region between the blade wakes
p	profile
u	tangential component
x	axial component
0	station upstream of blade row

3454

[redacted]

1 station just at blade trailing edge

2 station after mixing occurs

Superscript:

' absolute total state

[redacted]

APPENDIX B

DEVELOPMENT OF EQUATIONS USED IN MOMENTUM LOSS INVESTIGATION

The total-pressure loss due to mixing downstream of a blade row was obtained by satisfying continuity, momentum, and related conditions between stations 1 and 2 indicated in figure 1. The equations used are as follows:

Continuity. - At station 1,

$$w = \cos \alpha_1 \int_0^s \rho_1 V_1 du$$

At station 2,

$$w = s\rho_2 V_{x,2}$$

Thus,

$$\cos \alpha_1 \int_0^s \rho_1 V_1 du = s\rho_2 V_{x,2}$$

or, using stagnation conditions and specifying adiabatic flow,

$$\cos \alpha_1 \int_0^1 \left(\frac{\rho V}{\rho' V_{cr}}\right)_1 \frac{p_1'}{p_0'} d\left(\frac{u}{s}\right) = \left(\frac{\rho V_x}{\rho' V_{cr}}\right)_2 \frac{p_2'}{p_0'} \tag{B1}$$

Momentum in tangential direction. - The following equation relates the tangential momentum at stations 1 and 2:

$$\sin \alpha_1 \cos \alpha_1 \int_0^s \rho_1 V_1^2 du = s\rho_2 V_{x,2} V_{u,2}$$

or, using stagnation conditions,

$$\sin \alpha_1 \cos \alpha_1 \int_0^1 \left(\frac{\rho V^2}{\rho' V_{cr}^2}\right)_1 \frac{p_1'}{p_0'} d\left(\frac{u}{s}\right) = \left(\frac{\rho V_x V_u}{\rho' V_{cr}^2}\right)_2 \frac{p_2'}{p_0'} \tag{B2}$$

Momentum in axial direction. - The equation used in conserving momentum in the axial direction is more complicated than that used in the tangential direction, in that the change in static pressure must be considered. This equation is

$$gp_1 s + \cos^2 \alpha_1 \int_0^s \rho_1 V_1^2 du = gp_2 s + s\rho_2 V_{x,2}^2$$

Using stagnation conditions gives

$$\frac{gp_1}{\rho_0' V_{cr,0}^2} + \cos^2 \alpha_1 \int_0^1 \left(\frac{\rho V^2}{\rho' V_{cr}^2}\right)_1 \frac{p_1'}{p_0'} d\left(\frac{u}{s}\right) = \frac{gp_2}{\rho_0' V_{cr,0}^2} + \left(\frac{\rho V_x^2}{\rho' V_{cr}^2}\right)_2 \frac{p_2'}{p_0'} \tag{B3}$$

however,

$$\frac{gp_1}{\rho_0' V_{cr,0}^2} = \frac{gp_1 RT_0' (\gamma+1)}{p_0' \gamma g R T_0' 2} = \frac{p_1}{p_0'} \left(\frac{\gamma+1}{2\gamma}\right)$$

In the same manner,

$$\frac{gp_2}{\rho_0' V_{cr,0}^2} = \frac{p_2}{p_2'} \frac{p_2'}{p_0'} \left(\frac{\gamma+1}{2\gamma}\right)$$

Therefore, equation (B3) becomes

$$\frac{p_1}{p_0'} \left(\frac{\gamma+1}{2\gamma}\right) + \cos^2 \alpha_1 \int_0^1 \left(\frac{\rho V^2}{\rho' V_{cr}^2}\right)_1 \frac{p_1'}{p_0'} d\left(\frac{u}{s}\right) = \frac{p_2}{p_2'} \frac{p_2'}{p_0'} \left(\frac{\gamma+1}{2\gamma}\right) + \left(\frac{\rho V_x^2}{\rho' V_{cr}^2}\right)_2 \frac{p_2'}{p_0'} \tag{B4}$$

Additional relations. - Additional relations used in the analysis are:

(a) Isentropic pressure-velocity relation

$$\frac{p}{p'} = \left[1 - \frac{\gamma-1}{\gamma+1} \left(\frac{V}{V_{cr}}\right)^2\right]^{\frac{\gamma}{\gamma-1}} \tag{B5}$$

(b) Trigonometric velocity relation

$$\left(\frac{V}{V_{cr}}\right)^2 = \left(\frac{V_x}{V_{cr}}\right)^2 + \left(\frac{V_u}{V_{cr}}\right)^2 \tag{B6}$$

(c) Weight flow - velocity relation

$$\frac{\rho V_x}{\rho' V_{cr}} = \left[1 - \frac{\gamma-1}{\gamma+1}\left(\frac{V}{V_{cr}}\right)^2\right]^{\frac{1}{\gamma-1}} \frac{V_x}{V_{cr}} \tag{B7}$$

3454

These equations were used in the momentum loss analysis through an iteration process in the following manner:

(1) Ranges of $\frac{t}{s}$, $\left(\frac{V}{V_{cr}}\right)_{1,fs}$, and α_1 were specified. Thus, for any combination of these parameters, all conditions at station 1 are known.

(2) A series of $\frac{p_2'}{p_0'}$ was selected.

(3) The value of $\left(\frac{\rho V_x}{\rho' V_{cr}}\right)_2$ was calculated using equation (B1).

(4) The value of $\left(\frac{V_u}{V_{cr}}\right)_2$ was calculated using equation (B2).

(5) The value of $\left(\frac{V}{V_{cr}}\right)_2$ was obtained using equations (B6) and (B7) simultaneously.

(6) The value of $\left(\frac{p}{p'}\right)_2$ was computed using equation (B5).

(7) The value of $\frac{p_2'}{p_0'}$ was obtained using equation (B4).

When p_2'/p_0' assumed (step 2) is equal to that calculated (step 7), the solution for the specified stator exit conditions (step 1) is completed.

Additional parameters used in the text are:

(a) Mass-averaged total pressure at station 1

$$\left(\frac{p_1'}{p_0'}\right)_p = \frac{\int_0^1 \left(\frac{\rho V}{\rho' V_{cr}}\right)_1 \left(\frac{p_1'}{p_0'}\right)^2 d\left(\frac{u}{s}\right)}{\int_0^1 \left(\frac{\rho V}{\rho' V_{cr}}\right)_1 \frac{p_1'}{p_0'} d\left(\frac{u}{s}\right)} \tag{B8}$$

(b) Loss in terms of dynamic head. The loss in total pressure between stations 1 and 2 was also obtained in terms of free-stream dynamic head at station 1 through use of the following equations:

$$\bar{\omega}_1 = \frac{1 - \left(\frac{p_1'}{p_0'}\right)_p}{1 - \frac{p_1}{p_0'}} \tag{B9}$$

and

$$\bar{\omega}_2 = \frac{1 - \left(\frac{p_2'}{p_0'}\right)}{1 - \frac{p_1}{p_0'}} \tag{B10}$$

REFERENCES

1. Klapproth, John F.: General Considerations of Mach Number Effects on Compressor-Blade Design. NACA RM E53L23a, 1954.

2. Whitney, Warren J., Monroe, Daniel E., and Wong, Robert Y.: Investigation of Transonic Turbine Designed for Zero Diffusion of Suction-Surface Velocity. NACA RM E54F23, 1954.

3. Reeman, J., and Simonis, E. A.: The Effect of Trailing Edge Thickness on Blade Loss. Tech. Note No. 116, British R.A.E., Mar. 1943.

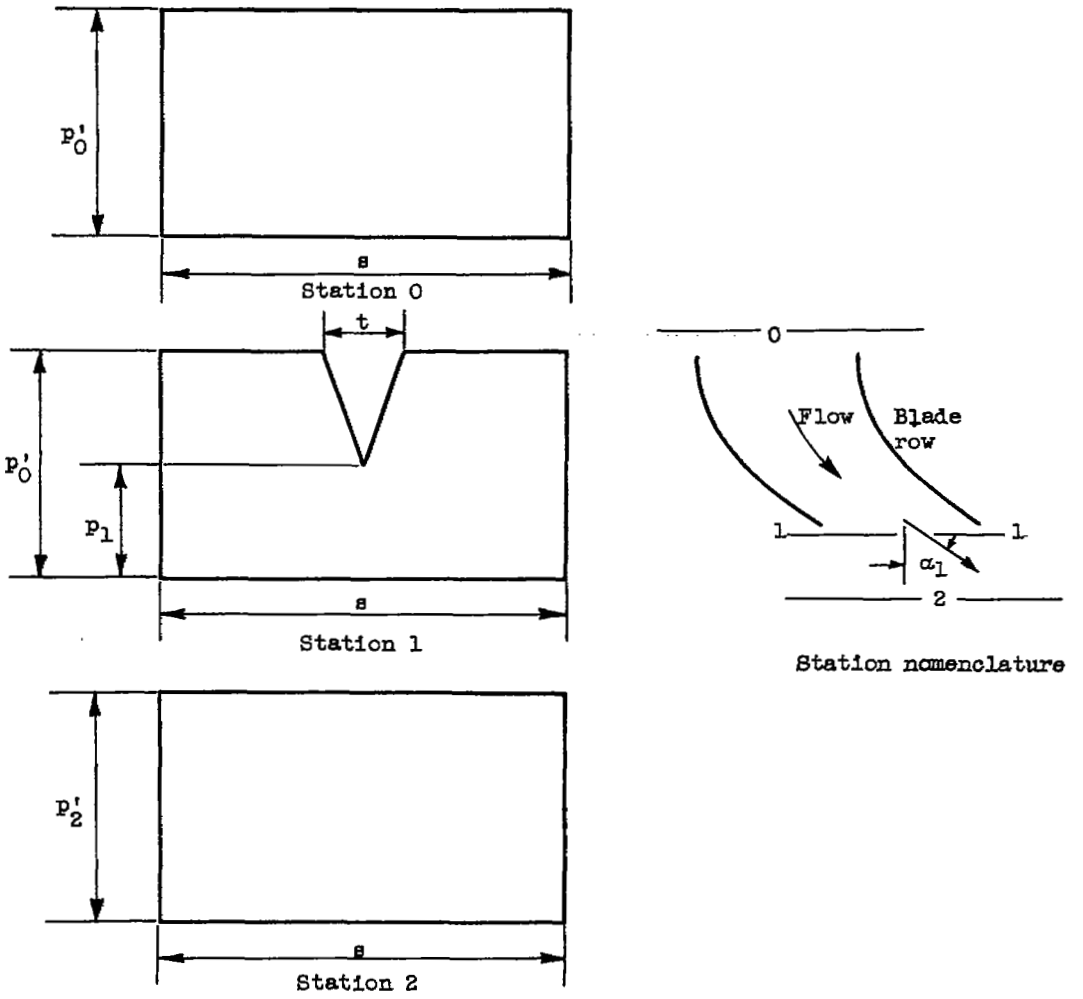

Figure 1. - Description of assumed total-pressure distribution at each station used in analysis of mixing loss.

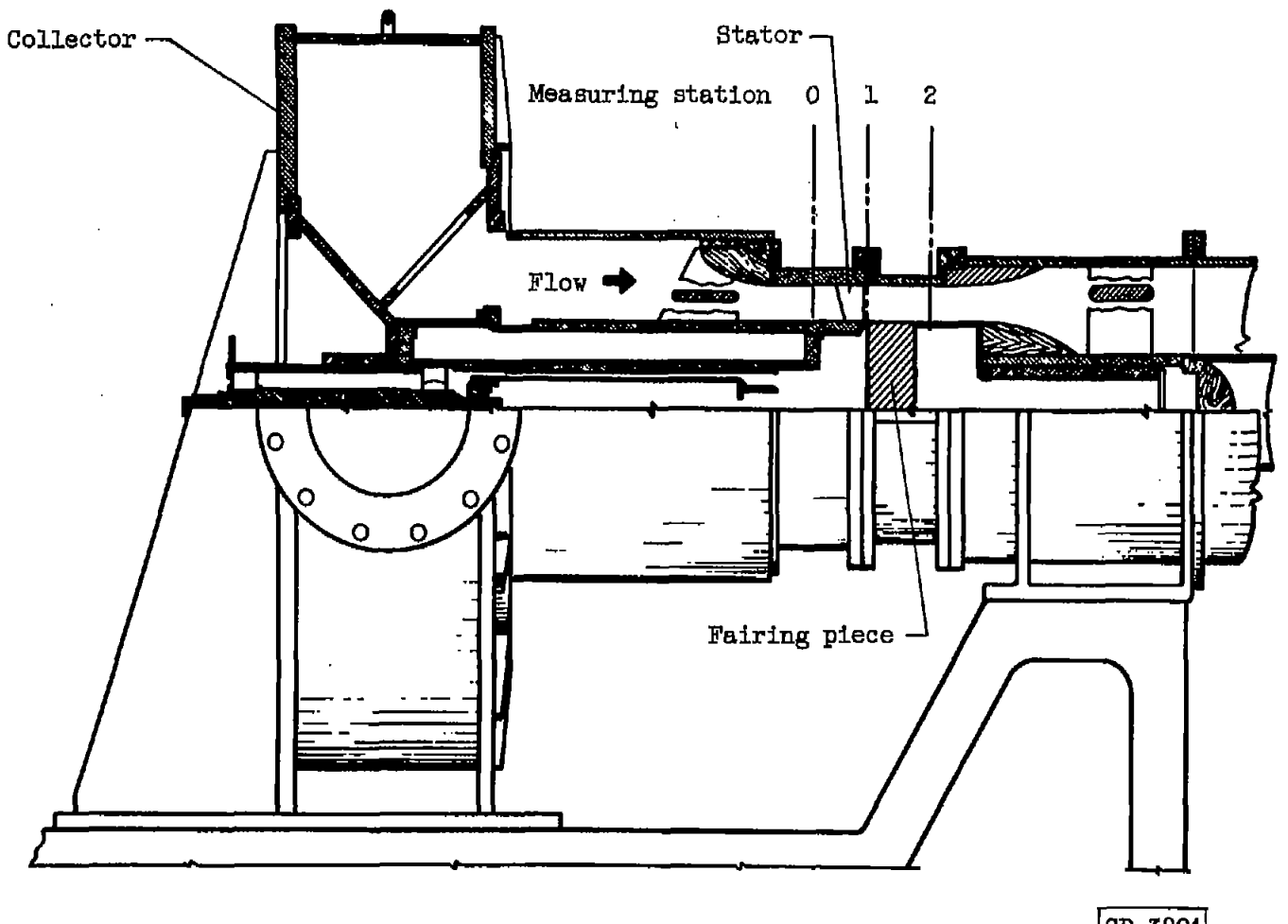

Figure 2. - Diagrammatic sketch of cold-air test section used in experimental investigation of mixing loss.

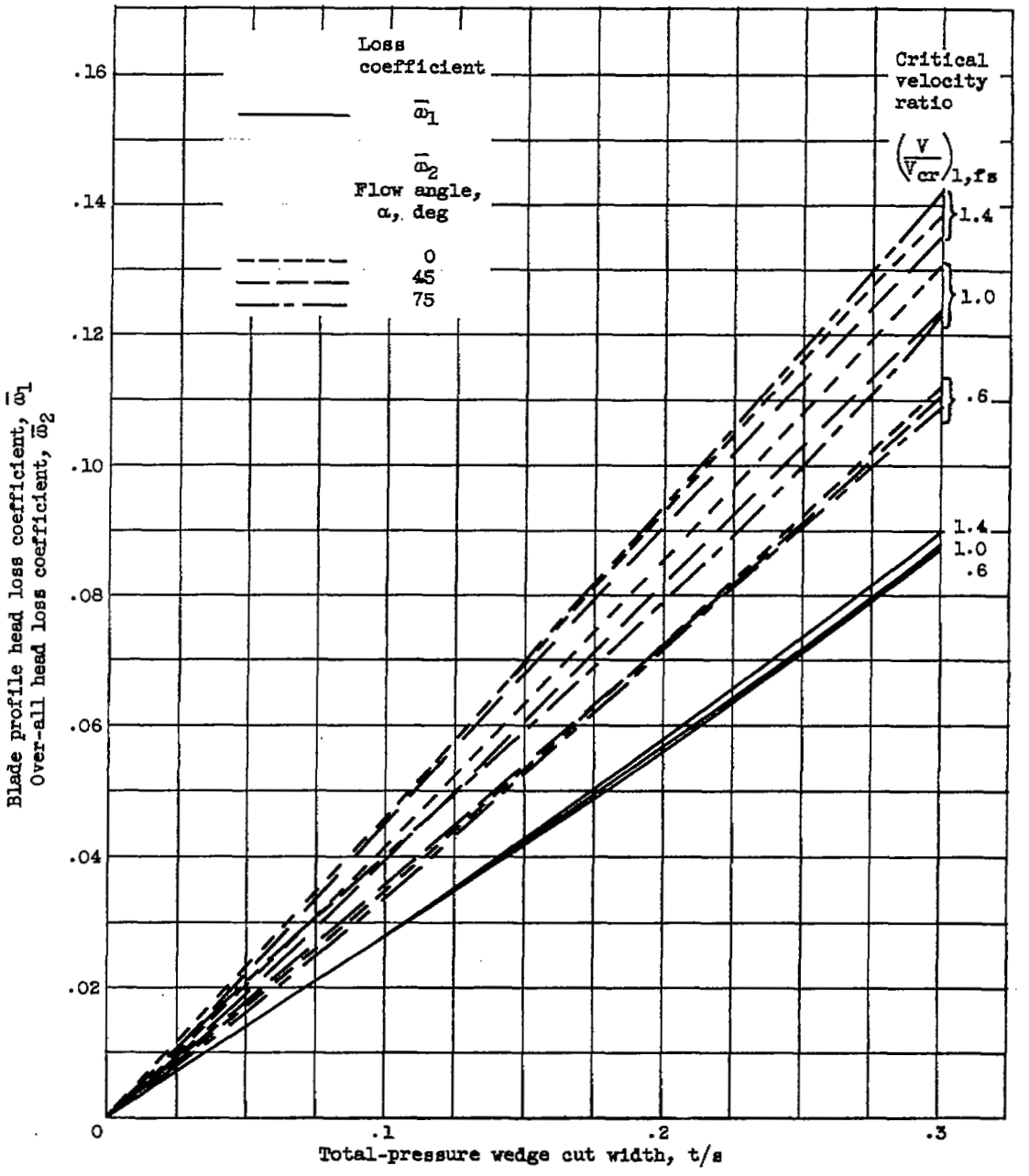

Figure 3. - Effect of mixing on head loss as indicated by analysis.

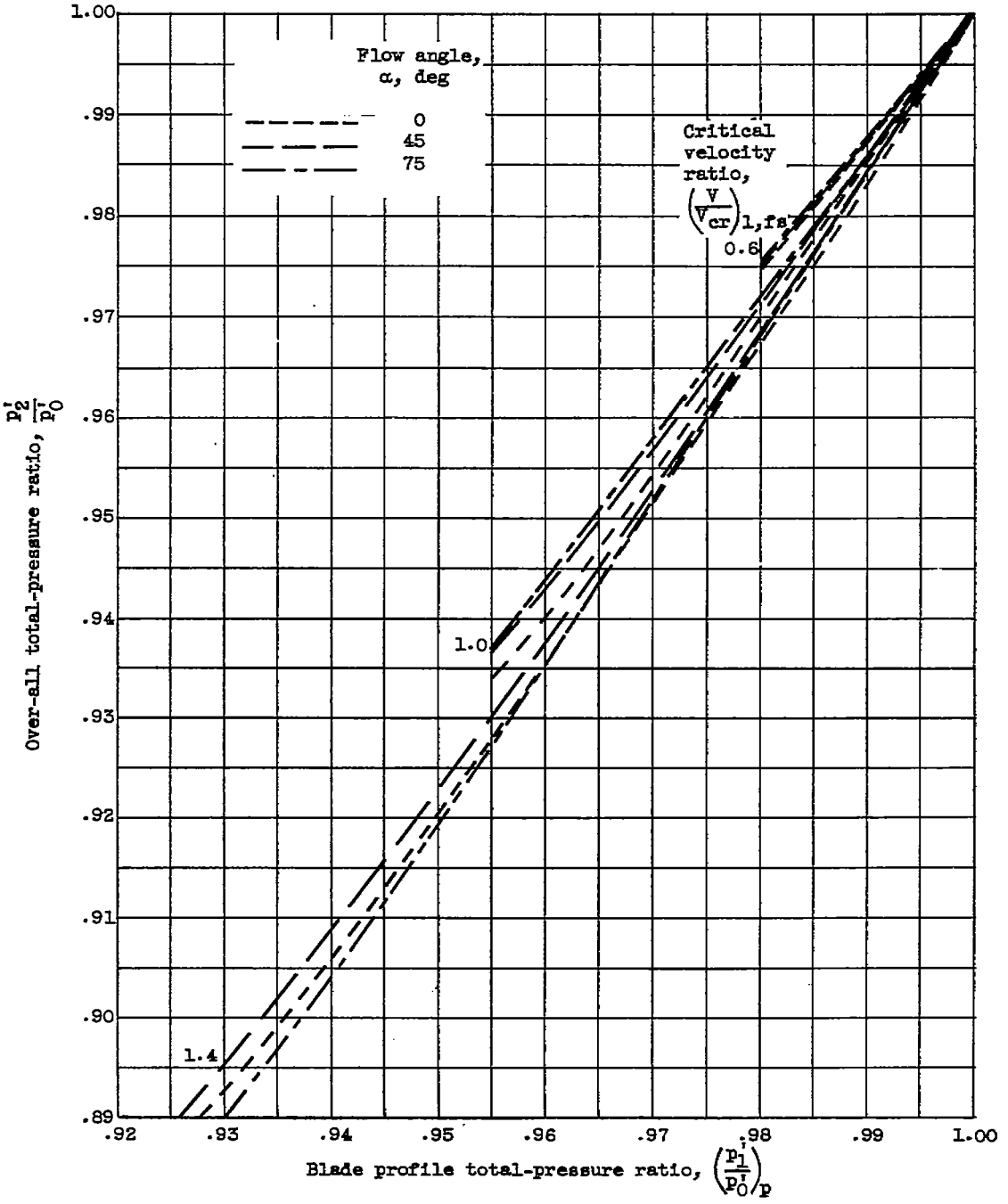

Figure 4. - Effect of mixing on total-pressure loss as indicated by analysis.

[redacted]

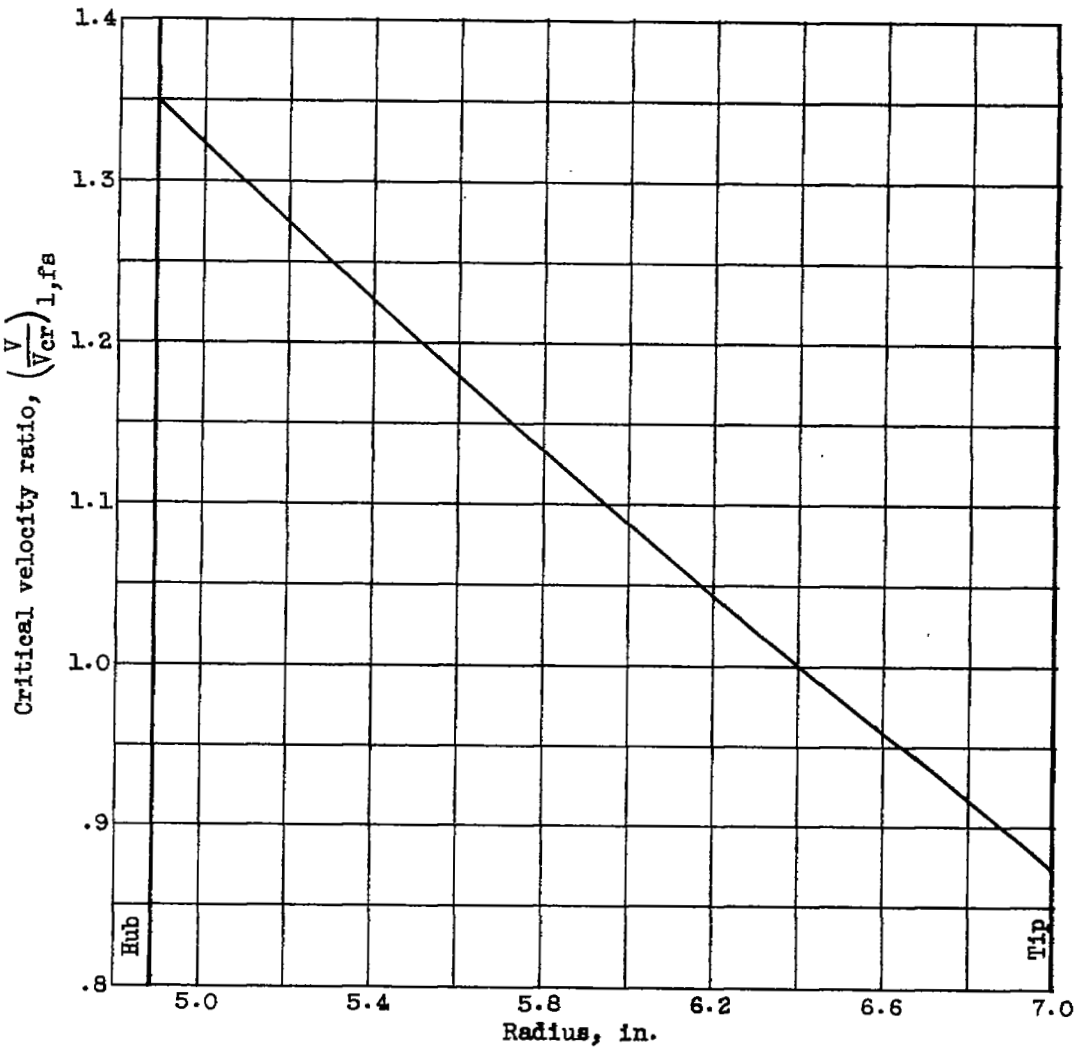

Figure 5. - Experimentally obtained free-stream velocity distribution just downstream of turbine stator.

[redacted]

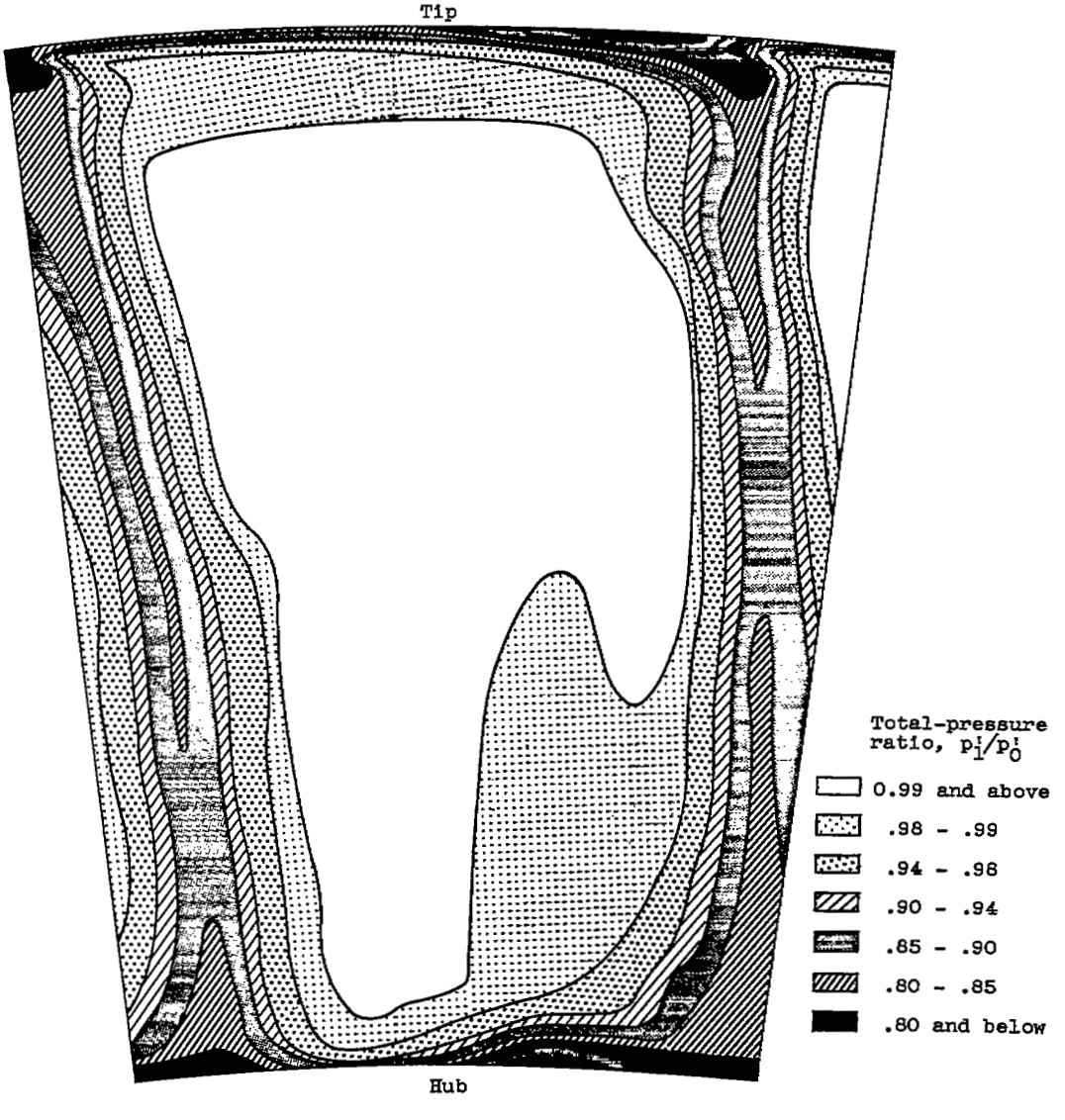

Figure 6. - Results of total-pressure survey at station 1.

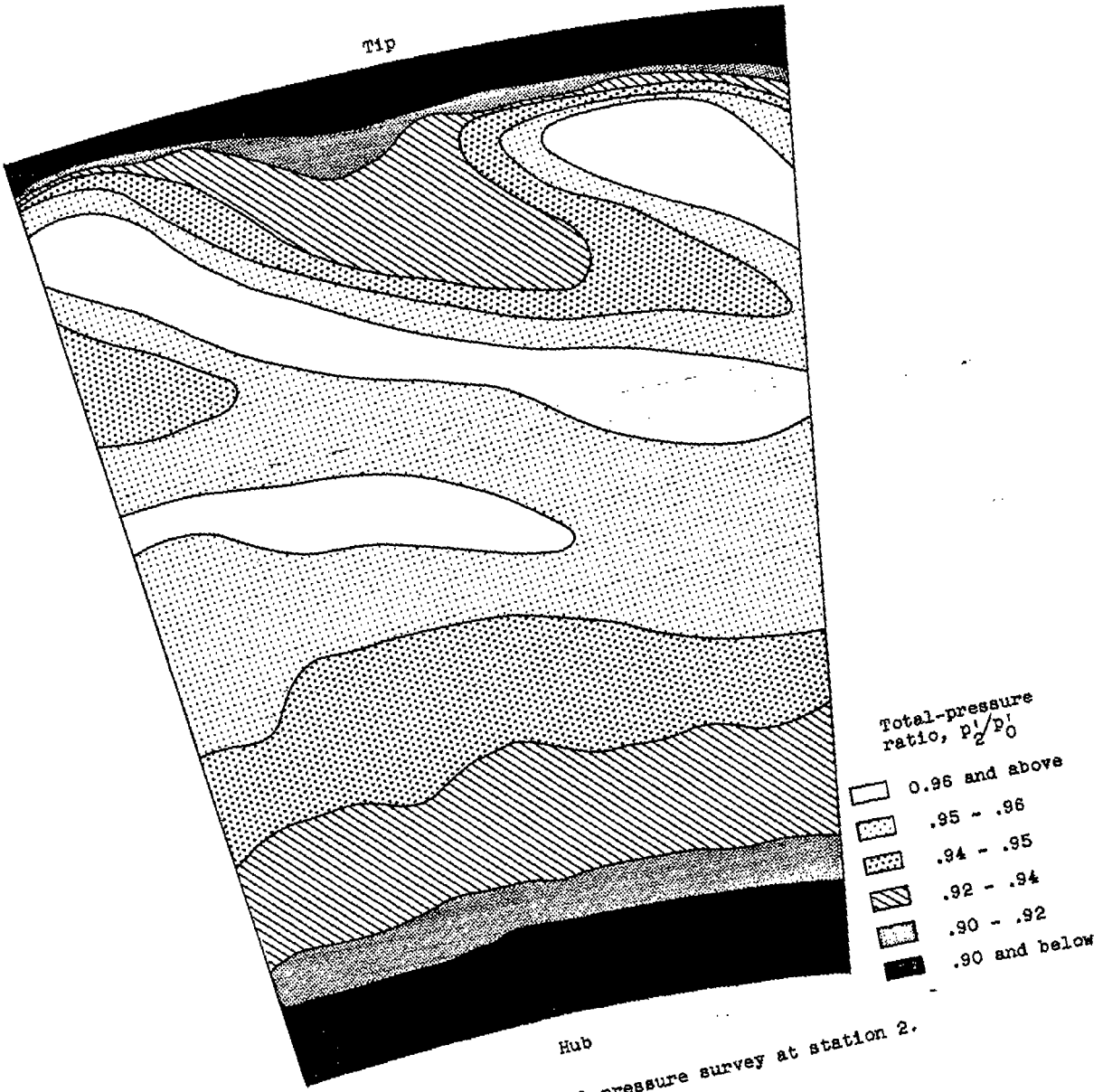

Figure 7. - Results of total-pressure survey at station 2.

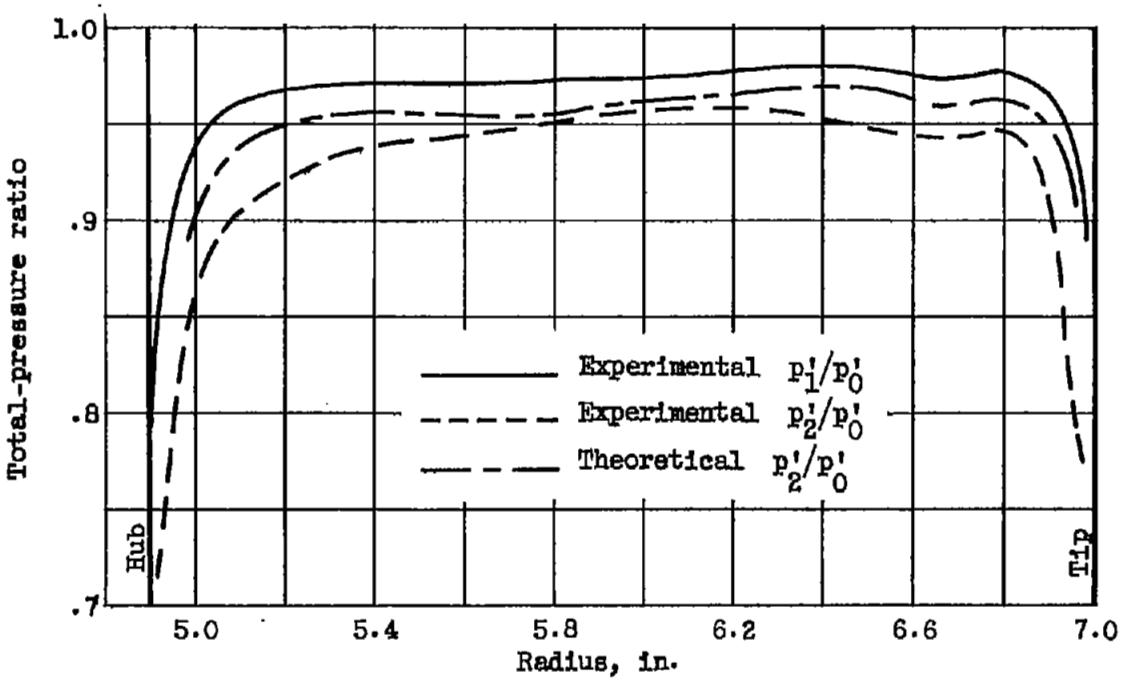

Figure 8. - Comparison between theoretical and experimental mixing losses obtained for turbine stator of reference 2.